Article

Cell Reports

Melanoma Suppressor Functions of the Carcinoma Oncogene FOXQ1

Graphical Abstract

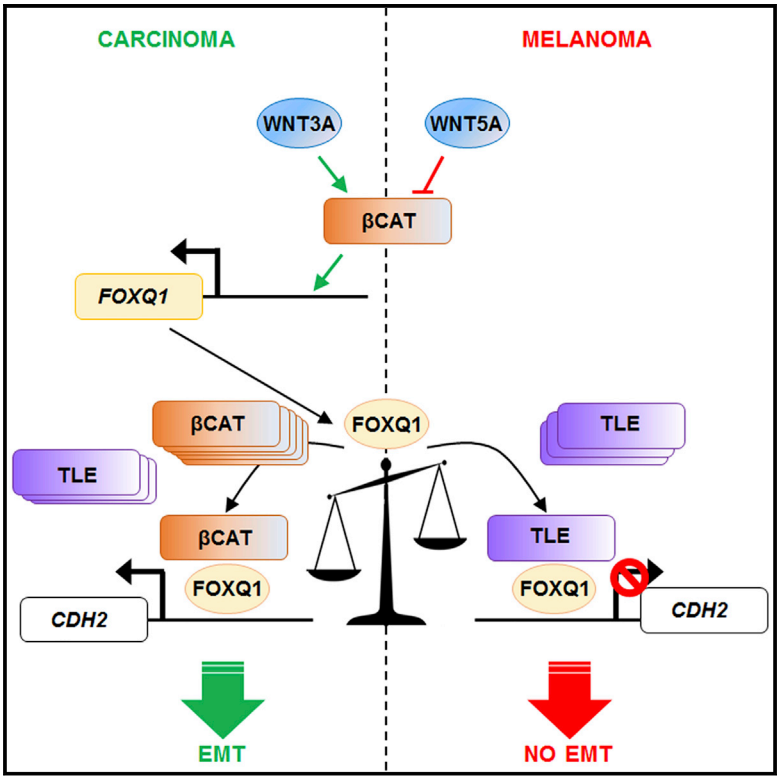

Authors

Archis Bagati, Anna Bianchi-Smiraglia, Sudha Moparthy, ..., Song Liu, Michael J. Nemeth, Mikhail A. Nikiforov

Correspondence

mikhail.nikiforov@roswellpark.org

In Brief

Bagati et al. report that the carcinoma oncogene FOXQ1 acts as a tumor suppressor in melanoma cells. Depending on β-catenin levels, which are higher in carcinoma than in melanoma cells, FOXQ1 activates or represses N-cadherin gene, invasion, and metastasis.

Highlights

- The carcinoma oncogene FOXQ1 suppresses invasion and metastasis in melanoma cells
- FOXQ1 inversely regulates N-cadherin gene (*CDH2*) in carcinoma and melanoma cells
- β-Catenin levels determine the mode of FOXQ1 regulation of *CDH2* and invasion

Accession Numbers

GSE103071

Bagati et al., 2017, Cell Reports *20*, 2820–2832
September 19, 2017
http://dx.doi.org/10.1016/j.celrep.2017.08.057

OPEN ACCESS
CellPress

Cell Reports
Article

Melanoma Suppressor Functions of the Carcinoma Oncogene FOXQ1

Archis Bagati,[1,7] Anna Bianchi-Smiraglia,[1] Sudha Moparthy,[1] Kateryna Kolesnikova,[1] Emily E. Fink,[1] Brittany C. Lipchick,[1] Masha Kolesnikova,[1] Peter Jowdy,[1] Anthony Polechetti,[1] Amin Mahpour,[2] Jason Ross,[1] Joseph A. Wawrzyniak,[1] Dong Hyun Yun,[1] Gyorgy Paragh,[1,3] Nadezhda I. Kozlova,[6] Albert E. Berman,[6] Jianmin Wang,[4] Song Liu,[4] Michael J. Nemeth,[5] and Mikhail A. Nikiforov[1,8,*]

[1]Department of Cell Stress Biology
[2]Department of Cancer Genetics
[3]Department of Dermatology
[4]Department of Biostatistics and Bioinformatics
[5]Department of Immunology
Roswell Park Cancer Institute, Buffalo, NY, USA
[6]Orekhovich Institute of Biomedical Chemistry, Moscow 119121, Russia
[7]Present address: Department of Cancer Immunology and Virology, Dana-Farber Cancer Institute, Harvard Medical School, Boston, MA 02215, USA
[8]Lead Contact
*Correspondence: mikhail.nikiforov@roswellpark.org
http://dx.doi.org/10.1016/j.celrep.2017.08.057

SUMMARY

Lineage-specific regulation of tumor progression by the same transcription factor is understudied. We find that levels of the FOXQ1 transcription factor, an oncogene in carcinomas, are decreased during melanoma progression. Moreover, in contrast to carcinomas, FOXQ1 suppresses epithelial-to-mesenchymal transition, invasion, and metastasis in melanoma cells. We find that these lineage-specific functions of FOXQ1 largely depend on its ability to activate (in carcinomas) or repress (in melanoma) transcription of the N-cadherin gene (*CDH2*). We demonstrate that FOXQ1 interacts with nuclear β-catenin and TLE proteins, and the β-catenin/TLE ratio, which is higher in carcinoma than melanoma cells, determines the effect of FOXQ1 on *CDH2* transcription. Accordingly, other FOXQ1-dependent phenotypes can be manipulated by altering nuclear β-catenin or TLE proteins levels. Our data identify FOXQ1 as a melanoma suppressor and establish a mechanism underlying its inverse lineage-specific transcriptional regulation of transformed phenotypes.

INTRODUCTION

Metastatic melanoma is one of the most deadly forms of cancer with rising incidence (Schadendorf et al., 2015; Shain and Bastian, 2016). The invasive and metastatic potential of melanoma cells is determined by their ability to undergo a process that resembles the epithelial to mesenchymal transition (EMT) (Alonso et al., 2007; Caramel et al., 2013; Tulchinsky et al., 2014). EMT underlies the acquisition of enhanced migratory and invasive properties by epithelial cells that are often associated with poor prognosis and a high risk of metastasis (Heerboth et al., 2015; Lamouille et al., 2014). Mechanistically, EMT is characterized by a cadherin switch, wherein the junctional adhesion protein E-cadherin (CDH1) is replaced by the neural subtype N-cadherin (CDH2) (Wheelock et al., 2008). This transition is orchestrated by a network of EMT transcription factors (EMT-TFs), including members of SNAI, ZEB, TWIST, and FOX families (Caramel et al., 2013; Lamouille et al., 2014). Although melanoma cells are not epithelial in nature, an EMT-like transition, including a cadherin switch, promotes melanoma invasion and metastasis (Alonso et al., 2007; Caramel et al., 2013; Li et al., 2015; Wheelock et al., 2008). Consistently, primary cutaneous melanomas that give rise to metastases demonstrate an increase in the mesenchymal marker N-cadherin and a decrease in the epithelial marker, E-cadherin, compared to tumors not progressing to metastases (Alonso et al., 2007).

In melanoma cells, lineage-specific microphthalmia-associated transcription factor (MITF), the master regulator of melanocytic differentiation and development, has also been characterized as a major suppressor of the EMT-like process and invasion (Bianchi-Smiraglia et al., 2017; Carreira et al., 2006; Hartman and Czyz, 2015; Hoek et al., 2008). Although the *MITF* gene has been reported to undergo amplification in ~15% of melanomas (Garraway et al., 2005), a significant body of literature demonstrates that strong downregulation of MITF, sometimes even below detection, correlates with poor prognosis and disease progression in patients (Carreira et al., 2006; Salti et al., 2000; Selzer et al., 2002; Wellbrock and Marais, 2005).

Previously, two carcinoma EMT-TFs (ZEB2 and SNAI2) have been demonstrated to suppress EMT in melanoma cells via transcriptional upregulation of MITF-associated differentiation. Yet the molecular factors regulating the EMT-like processes in melanoma cells independently of MITF or in cells with low or undetectable levels of MITF remain understudied.

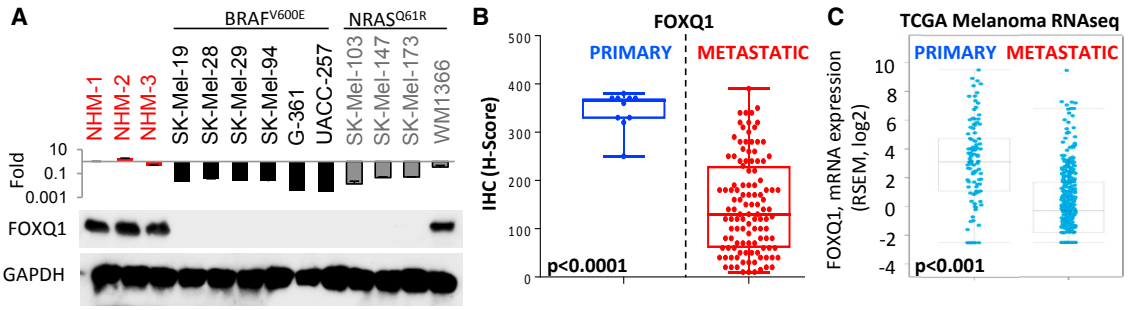

Figure 1. FOXQ1 Levels Decrease in Melanoma Progression

(A) Indicated cells were probed in qRT-PCR (*FOXQ1/ACTB* signal ratios are shown) (top) or in immunoblotting with the indicated antibodies (bottom).

(B) Expression of FOXQ1 in primary melanomas (individual tissue sections) and melanoma metastases (TMA). See the Supplemental Experimental Procedures for sample description and analysis.

(C) FOXQ1 mRNA expression (RSEM counts) in skin cutaneous melanoma TCGA database.

See also Figure S1.

Forkhead transcription factor FOXQ1, has been characterized as a major promoter of EMT, invasion, and metastasis in cells from several carcinomas including breast, colon, ovarian, and lung, where its levels correlate with poor prognosis (Li et al., 2016). FOXQ1 has been shown to exert oncogenic activity in large part by promoting the E/N cadherin switch (Zhang et al., 2011). Here, we report mechanisms underlying the ability of FOXQ1 to inhibit the same processes in melanoma cells.

RESULTS

FOXQ1 Expression Levels Decrease during Melanomagenesis

We were interested in identifying the expression pattern of FOXQ1 during melanoma progression. Surprisingly, we observed that the amounts of *FOXQ1* mRNA and protein were significantly decreased in cells from the vast majority of melanoma cell lines as compared to normal human melanocytes (NHM) (Figure 1A). Moreover, assessment of FOXQ1 expression in human melanoma specimens via immunohistochemistry demonstrated a statistically significant decrease in FOXQ1 levels in metastatic versus primary melanomas (Figures 1B and S1A). Consistently, analysis of the "TCGA cutaneous melanoma RNA-seq" dataset (https://cancergenome.nih.gov/) revealed a significant drop in *FOXQ1* mRNA levels in metastatic versus primary melanoma specimens (Figure 1C). Similarly, *FOXQ1* levels decreased in melanoma progression according to a separate gene expression database (Figure S1B, GSE4587) (Smith et al., 2005). Taken together these data suggest that, unlike in carcinoma progression, FOXQ1 expression levels decrease in melanoma progression.

FOXQ1 Negatively Affects Multiple Transformed Phenotypes in Melanoma Cells

To reveal the functional role of FOXQ1 downregulation, we restored its levels in cells from several melanoma cell lines approximately to the levels in NHM via lentiviral vector-based transduction of *FOXQ1* cDNA. This caused a wide spectrum of tumor suppressor phenotypes ranging from prominent inhibition of proliferation and induction of differentiation (SK-Mel-19, SK-Mel-29) (Figures 2A–2C), to a modest suppression of proliferation and a substantial decrease in invasion, tumorigenicity, and experimental metastasis (SK-Mel-103, SK-Mel-147, or Colo679) (Figures 2D–2I). Importantly, transduction of the same FOXQ1-expressing vector in breast (HMLER) or ovarian (SCOV3) carcinoma cells increased their invasion and enhanced tumorigenicity and experimental metastases over cells transduced with control vector (Figures S2A–S2G). Therefore, unlike in carcinoma cells, FOXQ1 induces tumor suppressor phenotypes in melanoma cells.

FOXQ1 Represses *CDH2* in Melanoma Cells with Various Levels of MITF

MITF is a major transcriptional repressor of melanoma cell invasion (Carreira et al., 2006). We were intrigued by the observation that FOXQ1 suppressed invasion in melanoma cells not expressing MITF protein (SK-Mel-103 and SK-Mel-147, Figure S3A). In carcinoma cells, FOXQ1 transcriptionally activates several genes involved in EMT (Qiao et al., 2011; Zhang et al., 2011; Meng et al., 2015) including those encoding ZEB2, TWIST1, vimentin, and N-cadherin (CDH2) and represses transcription of E-cadherin (*CDH1*) gene. Therefore, we assessed the levels of these proteins in SK-Mel-103 and SK-Mel-147 cells transduced with empty vector or FOXQ1-expressing vector. Levels of TWIST1, ZEB2, and vimentin remained unchanged, whereas E-cadherin levels were undetectable in these cells (Figure 3A). Therefore, the above proteins are unlikely to account for FOXQ1 tumor suppressor functions in melanoma cells. At the same time, these genes demonstrated FOXQ1-dependent pattern of regulation in carcinoma cells, consistent with FOXQ1 role in carcinoma (Figure 3A).

Paradoxically, ectopic expression of FOXQ1 uniformly suppressed *CDH2* mRNA and protein levels in all tested melanoma cells (Figures 3A–3C), independently of their MITF levels (Figure S3A). Reciprocally, small hairpin RNA (shRNA)-mediated depletion of FOXQ1 in a Colo-679 human melanoma cells expressing low but detectable levels of FOXQ1 increased *CDH2* mRNA and protein levels compared to control shRNA cells

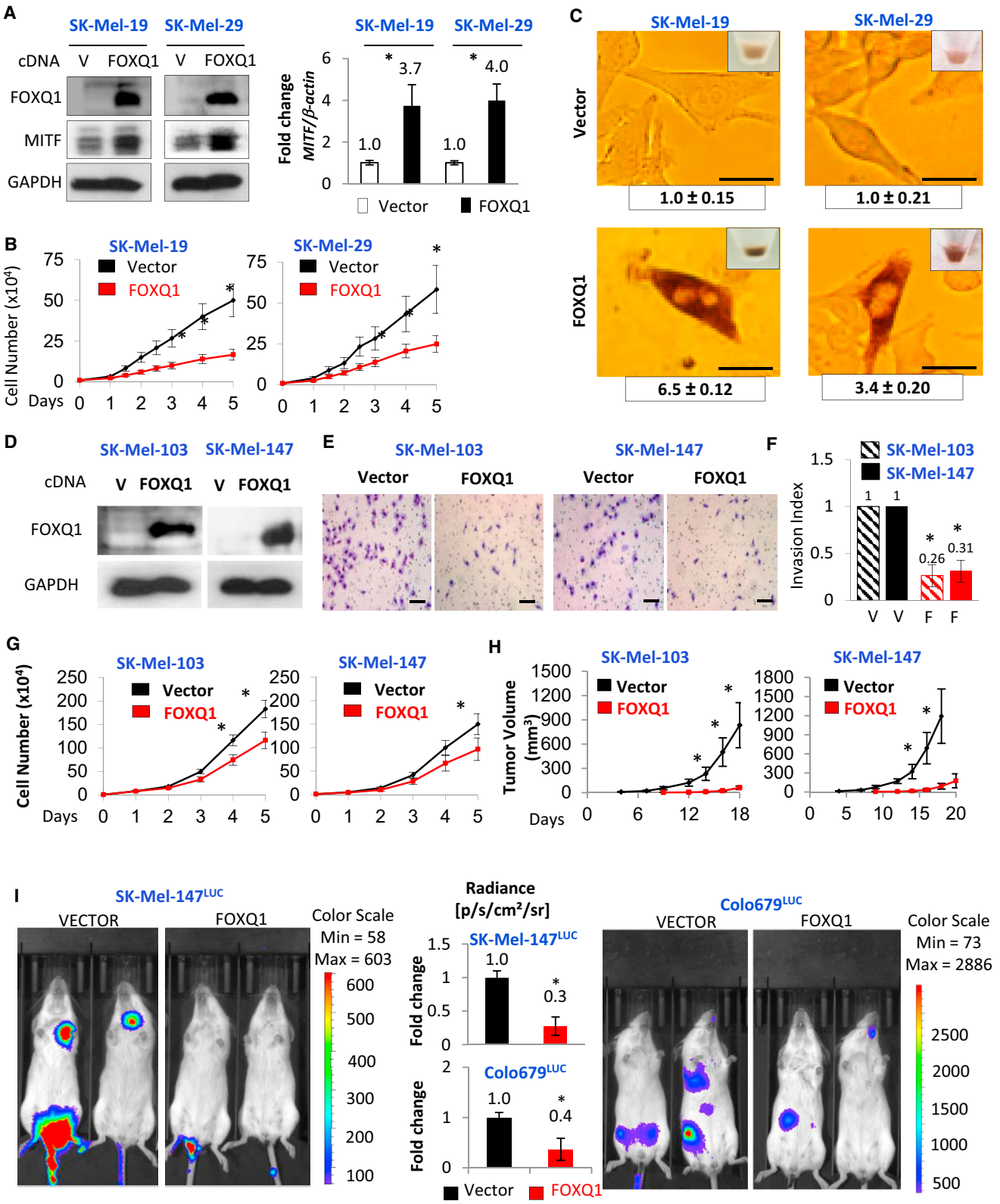

Figure 2. FOXQ1 Exerts Tumor Suppressive Phenotypes in Melanoma

(A) Cells transduced with the indicated constructs were probed in immunoblotting with the indicated antibodies (left) or in qRT-PCR with indicated primers (right).

(B) Cells described in (A) were counted daily starting 48 hr after infection.

(legend continued on next page)

(Figures 3D and 3E). In contrast, using the same genetic constructs, we reproduced previously published findings that FOXQ1 overexpression upregulates, whereas its depletion decreases *CDH2* mRNA and protein levels in carcinoma cells including HeLa, HMLE, HMLER, and SCOV3 (Figures S3B–S3D).

To investigate whether FOXQ1 is also capable of suppressing N-cadherin levels and invasion in cells with acutely depleted MITF, we transduced SK-Mel-28 melanoma cells in parallel with control or two MITF-specific shRNAs, followed by superinfection with empty vector or vector expressing FOXQ1. As shown in Figure S3E, depletion of MITF did not substantially affect the ability of FOXQ1 to suppress N-cadherin levels. Accordingly, FOXQ1 suppressed invasion in MITF-depleted SK-Mel-28 cells to a similar degree as in control SK-Mel-28 cells (Figure S3F). Collectively, these observations suggest that FOXQ1 suppresses invasion predominantly in MITF-independent manner.

To further evaluate cell-type-specific pattern of *CDH2* transcriptional control by FOXQ1, we tested its ability to regulate *CDH2* promoter-driven transcription in a luciferase reporter assay in carcinoma and melanoma cells. To this end, we cloned the (−2,200: 500 bp) region of human *CDH2* gene into pGL3-basic vector (pGL3-CDH2). This construct, in parallel with empty pGL3-basic vector, was co-transfected in combination with empty expression vector or FOXQ1-expressing vector into melanoma (SK-Mel-103, SK-Mel-147) or carcinoma (SCOV3 and HMLER) cells. We demonstrated that FOXQ1 respectively induced or suppressed activity of exogenous *CDH2* promoter in carcinoma and melanoma cells (Figures 3F and 3G). Therefore, collectively, our data suggest that FOXQ1 oppositely regulates *CDH2* gene expression in a lineage-specific manner.

FOXQ1 Interacts with β-Catenin and TLE Proteins in Melanoma and Carcinoma Cells

To determine whether FOXQ1 binds to the *CDH2* promoter at the same binding sites in melanoma and carcinoma cells, we performed chromatin immunoprecipitation (ChIP) assay using FLAG antibodies in melanoma (SK-Mel-103, −147) and carcinoma (HMLER and SCOV3) cells transduced with either control vector or FLAG-FOXQ1-expressing vector. Our analyses identified similar enrichment patterns of *CDH2* promoter regions in materials precipitated with FLAG antibodies from both carcinoma and melanoma cells expressing FLAG-FOXQ1, but not control cells (Figures 3H and 3I). These data suggest that FOXQ1 interacts with the same binding sites in the promoter of *CDH2* gene in both cell lineages.

To further characterize lineage-specific regulation of *CDH2* by FOXQ1, we performed ChIP assays in melanoma (SK-Mel-147) and carcinoma (SCOV3) cells transduced with FOXQ1 cDNA or empty-vector. Control IgG antibodies or antibodies to the following proteins were utilized: RNA polymerase II (RNA pol II), markers of actively transcribed chromatin (histone H3 acetylated at lysine 9 [H3K9AC] and histone H3 tri-methylated at lysine 4 [H3K4Me3]), and markers of repressive chromatin (histone H3 di-methylated at lysine 9 [H3K9Me2] and histone H3 tri-methylated at lysine K27 [H3K27Me3]). DNA precipitated in the above assays was probed in quantitative PCR with primers corresponding to FOXQ1 binding sites 1 and 2 in *CDH2* promoter (Figure 3H). As shown in Figure S3G, markers of repressive chromatin and permissive chromatin were, respectively, more and less prevalent at *CDH2* promoter in FOXQ1-expressing melanoma cells compared to control melanoma cells transduced with empty vector. Accordingly, RNA Polymerase II interacted less efficiently with *CDH2* promoter in FOXQ1-expressing cells than control cells. Overexpression of FOXQ1 in carcinoma cells led to exactly opposite results (Figure S3G).

We hypothesized that lineage-specific transcriptional regulation of *CDH2* by FOXQ1 may depend on co-factor(s) differentially interacting with FOXQ1 in melanoma and carcinoma cells. TCF/LEF transcription factors represent a classic example of co-factor-dependent mode of transcription regulation. TCF/LEF proteins interact with groucho/TLE transcription repressors resulting in suppression of downstream genes (Roose et al., 1998). Nuclear β-catenin displaces groucho/TLEs thus allowing transcription activation by TCF/LEF (Daniels and Weis, 2005). Additionally, melanoma cells possess reduced levels of nuclear β-catenin (Biechele et al., 2012; Kuphal and Bosserhoff, 2011).

To identify the role of β-catenin in FOXQ1-dependent processes, we first demonstrated that the studied melanoma cells contained lower amounts of nuclear β-catenin than carcinoma cells (Figure 4A) in agreement with previous findings (Biechele et al., 2012; Kuphal and Bosserhoff, 2011). We did not detect a uniform difference in the levels of nuclear TLEs proteins between melanoma and carcinoma cells (Figure 4A). Next, we probed several melanoma and carcinoma cells in a TOP/FOP assay, a well-established method for detecting β-catenin activity in a cell. Melanoma cells were less active in a TOP/FOP assay than carcinoma cells (Figure 4B), as it has been previously reported (Biechele et al., 2012; Kuphal and Bosserhoff, 2011). Levels of AXIN2, a bona fide marker of activated β-catenin pathway were generally lower in melanoma than carcinoma cells (Figure S4A).

To determine whether FOXQ1 interacts with β-catenin and/or TLE proteins, empty vector or FLAG-FOXQ1-expressing vector

(C) Representative images of cells described in (A). Images were taken 96 hr after infection. Scale bars, 50 μm.
(D) Cells expressing vector (V) or FOXQ1 were probed in immunoblotting with the indicated antibodies.
(E) Representative images of cells described in (D) after completion of Boyden invasion chambers assay. Scale bars, 200 μm.
(F) Quantification of (E).
(G and H) Cells described in (D) were (G) counted at indicated days or (H) subjected to tumorigenicity assay in SCID mice (n = 5).
(I) SK-Mel-147^{LUC} and Colo679 ^{LUC} cells stably expressing luciferase were transduced with the indicated constructs and tail-vein injected into SCID mice (n = 6). Mice were assayed for bioluminescence via IVIS 3 weeks post-injection. Representative images shown, Bar diagram demonstrates data quantification. All data represent mean ± SEM. Statistical significance was assessed using two-tailed Student's t tests. A $p < 0.05$ (*) was considered significant.
See also Figure S2.

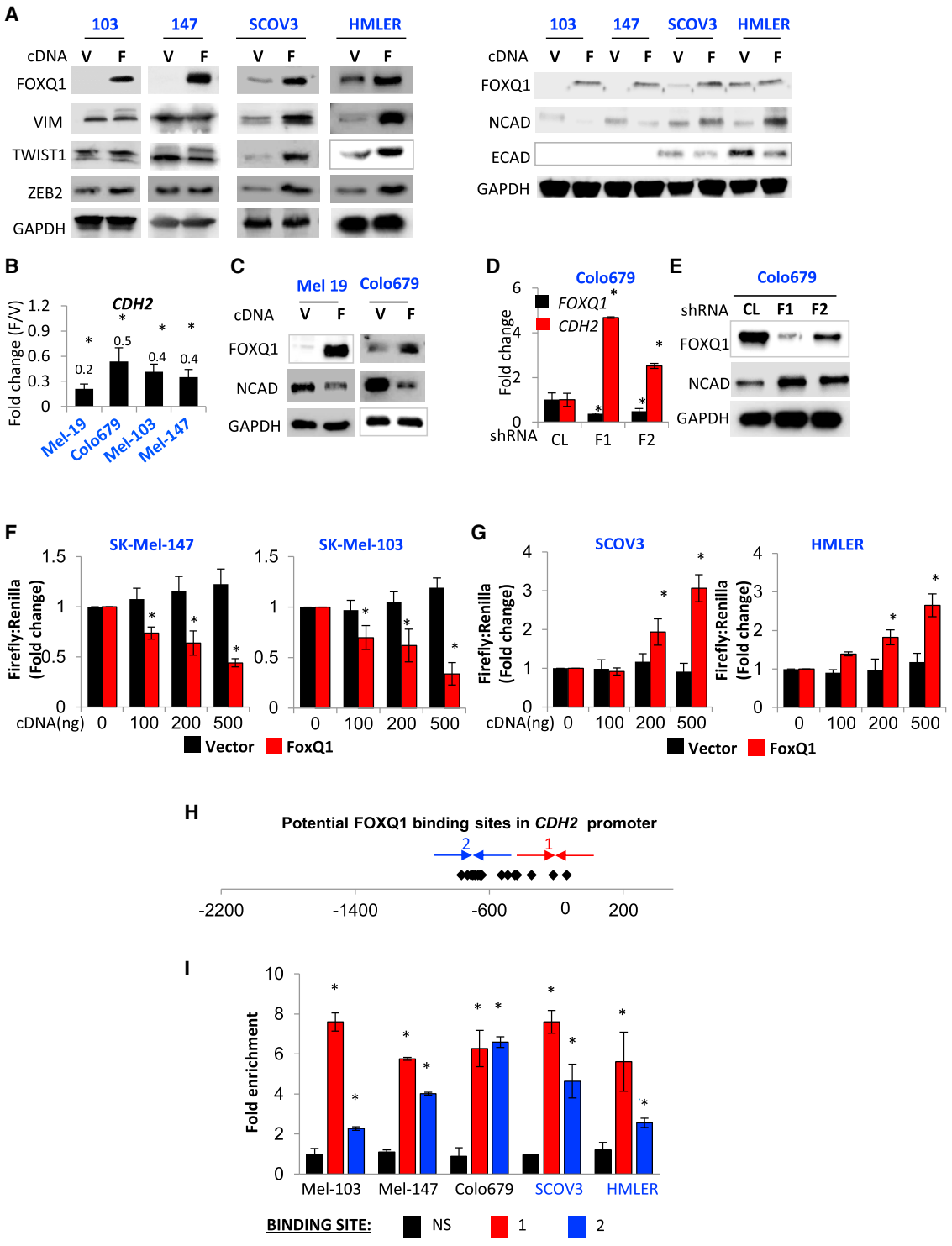

Figure 3. FOXQ1 Differentially Regulates *CDH2* in Melanoma and Carcinoma Cells

(A) Cells transduced with the vector (V) or FOXQ1 (F) were probed in immunoblotting with indicated antibodies.

(B) *CDH2/ACTB* qRT-PCR signals obtained in cells transduced with FOXQ1 cDNA (F) were normalized by corresponding qRT-PCR signals obtained in cells transduced with empty vector (V).

(C) Indicated melanoma cells were treated like in (A).

(D) Cells were transduced with control (CL) or FOXQ1 (F1, F2) shRNAs and probed in qRT-PCR with indicated primers (*FOXQ1/ACTB* and *CDH2/ACTB* signal ratios are shown).

(legend continued on next page)

were transduced into SK-Mel-147 cells followed by preparation of nuclear extracts and immunoprecipitation with FLAG-specific antibodies. The precipitated materials were probed in immunoblotting with β-catenin or pan-TLE antibodies (Figure 4C). We detected a substantial enrichment of endogenous β-catenin and TLE proteins in material precipitated with FLAG antibodies from FLAG-FOXQ1-expressing cells compared to control cells (Figure 4C). Reciprocally, materials co-precipitated with endogenous β-catenin or TLE proteins from nuclear extracts of FLAG-FOXQ1-expressing cells were enriched with FOXQ1 as compared to materials precipitated with IgG (Figures 4D and 4E). In addition, we observed similar results with regard to FOXQ1 interaction with β-catenin and TLEs in transient co-transfection experiments in HEK293T cells (Figures S4B and S4C).

To assess interactions between endogenous FOXQ1, β-catenin, and TLEs proteins, we performed reciprocal co-immunoprecipitations with control IgG antibodies or antibodies specific to the above proteins from nuclear extracts of SCOV3 cells. We demonstrated that similarly to exogenously expressed FOXQ1 in melanoma cells, endogenous FOXQ1 co-immunoprecipitated β-catenin and TLEs in carcinoma cells (Figures 4F–4H).

To confirm that FOXQ1 recruits β-catenin and/or TLE to *CDH2* promoter, we performed ChIP in SK-Mel-147-FLAG-FOXQ1 cells using FLAG or TLE antibodies and in uninfected SCOV3 cells using FOXQ1 or β-catenin antibodies. IgG antibodies were used as a negative control. As shown in Figure 4I, DNA regions containing FOXQ1 binding sites in *CDH2* promoter were enriched in the material precipitated with FLAG or TLE antibodies in melanoma cells and with FOXQ1 or β-catenin antibodies in carcinoma cells.

Next, to determine whether β-catenin affects TLE binding to *CDH2* promoter in melanoma cells, we performed ChIP with IgG, FLAG, β-catenin, and TLEs antibodies in SK-Mel-147 cells overexpressing FLAG-FOXQ1 alone or in combination with EβP. As shown in Figure 4J, DNA regions containing FOXQ1 binding sites in *CDH2* promoter were enriched in material precipitated with FLAG or TLE antibodies (but not control IgG). Overexpression of EβP in these cells resulted in increased enrichment of *CDH2* DNA in material precipitated with β-catenin antibodies, did not affect such enrichment in materials precipitated FLAG-antibodies (i.e., FOXQ1), but decreased the *CDH2* DNA enrichment in materials precipitated with TLE antibodies. We therefore concluded that β-catenin does not affect FOXQ1 DNA binding but decreases TLE DNA binding presumably via disrupting FOXQ1/TLE interactions and ultimately leading to alleviation of *CDH2* transcriptional repression.

Taken together, these results strongly argue for FOXQ1 physical interactions with β-catenin and TLE proteins.

FOXQ1 Inhibits Melanoma Cell Invasion Mainly via Repression of *CDH2*

We were interested in whether other genes involved in invasion-associated processes are controlled by FOXQ1 in melanoma and carcinoma cells similarly to *CDH2*. To this end, we performed RNA sequencing (RNA-seq) analysis in SK-Mel-147 and SCOV3 cells transduced with empty or FOXQ1-expressing vectors. We identified 784 genes that were suppressed by FOXQ1 at least 1.5-fold in melanoma cells and at the same time upregulated by FOXQ1 at least 1.5-fold in carcinoma cells (19.4% of all FOXQ1-suppressed genes in melanoma cells and 9.4% of all FOXQ1-upregulated genes in carcinoma cells, respectively). This gene list was overlapped with the list of β-catenin target genes identified via ChIP-seq methodology (Sequence Read Archive: SRA012054). Thus, 36 genes were identified, 13 of which have been previously reported to increase invasion-associated phenotypes in carcinoma cells (Table S1). For each of these 13 genes, we identified FOXQ1-dependent activation in SCOV3 cells and FOXQ1-dependent suppression in SK-Mel-147 via qRT-PCR (Figure S4D).

The above data suggest that FOXQ1-dependent invasion in melanoma cells could be mediated by multiple genes. Therefore, we wanted to establish an individual role of *CDH2* in FOXQ1-dependent regulation of invasion. To this end, we ectopically expressed *CDH2* cDNA in SK-Mel-103 and SK-Mel-147 cells via lentiviral infection achieving ~2-fold increase in the total amounts of N-cadherin. These cells were super-infected with empty vector or a FOXQ1 cDNA expressing vector (Figure 4K). Restoration of N-cadherin levels in FOXQ1-expressing melanoma cells abrogated the ability of FOXQ1 to suppress invasion by ~50%–70% (Figures 4L and 4M), suggesting that downregulation of N-cadherin mediates in large part the invasion-suppressing activity of FOXQ1.

β-Catenin and TLEs Determine the Mode of FOXQ1-Dependent Regulation of *CDH2*

To evaluate the role of β-catenin in FOXQ1-dependent regulation of *CDH2* gene in melanoma cells, we increased the nuclear levels of β-catenin in SK-Mel-103 and SK-Mel-147 cells via lentivirus-based expression of constitutively active S33Y β-catenin mutant (EβP). The obtained cell populations were super-infected with control or FOXQ1-containing lentiviral vectors, followed by assessment of *CDH2* mRNA and protein levels. Expression of EβP in SK-Mel-103 and SK-Mel-147 melanoma cells prevented FOXQ1-mediated repression of *CDH2* mRNA and protein levels (Figures 5A and 5B).

In parallel, we performed experiments in HMLER and SCOV3 cells, where shRNA-mediated depletion of β-catenin was carried out with concomitant FOXQ1 overexpression. Depletion of

(E) Cells described in (D) were probed in immunoblotting with the indicated antibodies.
(F and G) Melanoma (F) or carcinoma (G) cells were co-transfected with either pGL3-basic (black) or pGL3-CDH2 (red) vectors and the indicated amounts of FOXQ1 cDNA or empty vector, and assayed for luciferase activity.
(H) *CDH2* promoter. Shown are FOXQ1 binding sites (diamonds) and PCR primers (arrows).
(I) ChIP assay. qPCR signals in reactions with DNA precipitated with FLAG antibodies from FLAG-FOXQ1-cells were normalized by corresponding signals in vector cells and by the signal obtained with *CDH2* non-specific control primers (NS). Black, red, and blue bars correspond to FOXQ1 non-specific DNA region, FOXQ1 binding regions "1," and "2," respectively.
See also Figure S3.

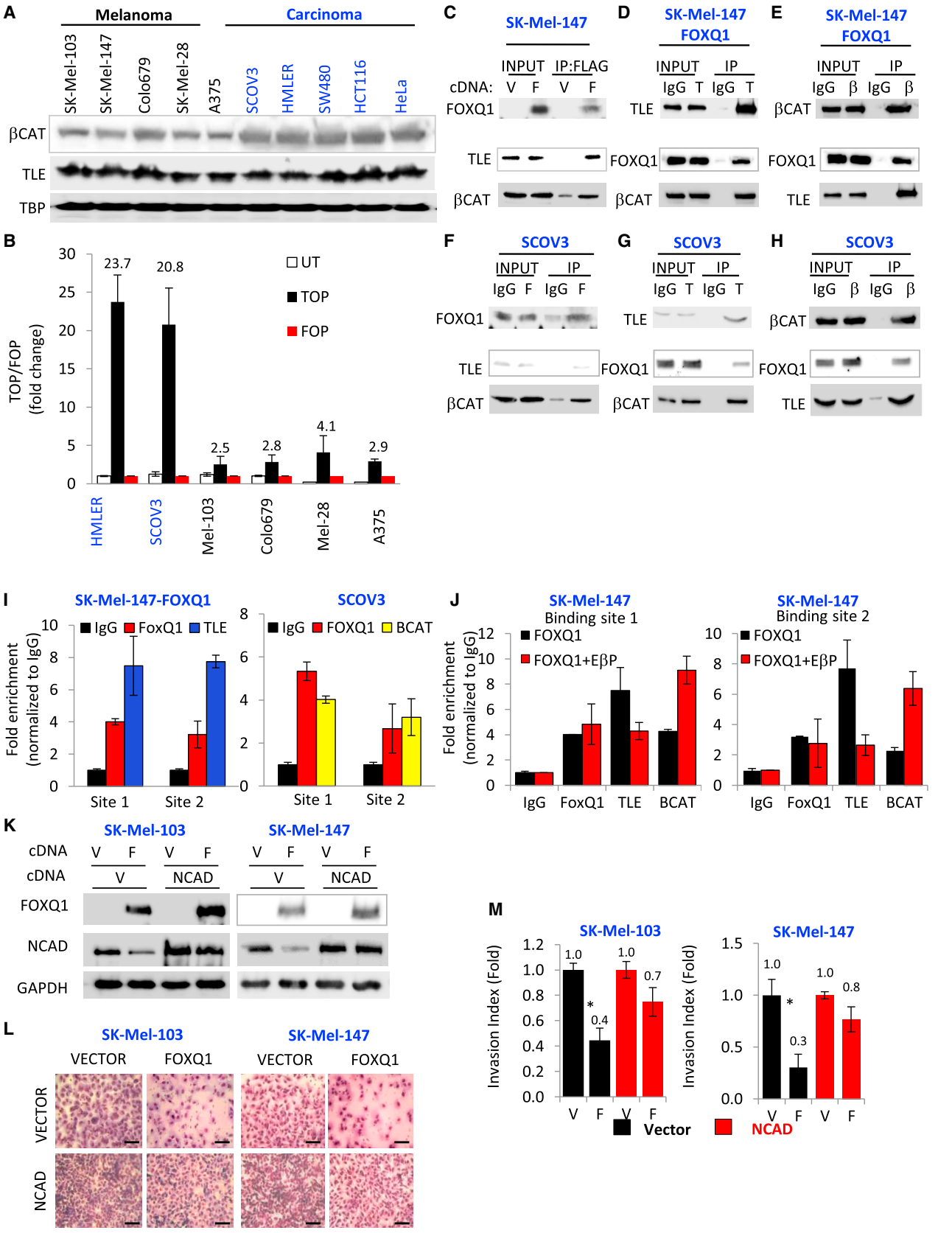

(legend on next page)

β-catenin decreased endogenous FOXQ1 (in agreement with previously published data) (Christensen et al., 2013; Peng et al., 2015) and N-cadherin levels (Figures 5C and 5D). Importantly, ectopic expression of FOXQ1, while compensating for downregulation of endogenous FOXQ1, was still unable to significantly upregulate N-cadherin levels when β-catenin was depleted (Figures 5C and 5D) further supporting our model. Similarly, opposite results with regard to FOXQ1 regulation of *CDH2* in melanoma and carcinoma cells were obtained in luciferase reporter assay using the control and *CDH2* promoter-containing pGL3 vectors (Figures 5E and 5F).

β-Catenin Regulates FOXQ1-Dependent Invasion and Metastasis

To determine whether β-catenin affects FOXQ1-dependent suppression of invasion, vector or EβP-expressing SK-Mel-103 and SK-Mel-147 cells were super-infected with control or FOXQ1-containing lentiviral vectors followed by assessment of invasion potential (Figure 5G).

Interestingly, ectopic expression of activated β-catenin by itself suppressed invasion in melanoma cells by 30%–50% (Figure 5G). This was in agreement with previous reports on β-catenin invasion-inhibiting activity in melanoma cells (Domingues et al., 2014, 2017; Rambow et al., 2016). On the other hand, co-expression of FOXQ1 and EβP negated each other invasion-suppressing activities (Figure 5G). The ability of FOXQ1 to suppress invasion (and N-cadherin levels) was also blunted by small interfering RNA (siRNA)-mediated depletion of TLE proteins (Figures S5A and S5B) further supporting our model of FOXQ1 function in melanoma cells.

To establish whether the FOXQ1-dependent control of metastatic potential in melanoma cells is also affected by β-catenin, SK-Mel-147-Luc cells were transduced with the following combination of vectors: two empty vectors, vector and FOXQ1, vector and EβP, or EβP and FOXQ1, and injected via the tail vein into SCID mice. The animals were monitored for luciferase activity using the IVIS imaging platform. FOXQ1-expressing melanoma cells demonstrated suppressed metastasis compared to empty-vector cells (Figure 5H). Similar to invasion assay, EβP suppressed experimental metastasis of SK-Mel-147-Luc cells but reverted the suppression of metastasis by FOXQ1 (Figure 5H). Therefore, our data strongly suggest that although β-catenin demonstrates tumor-suppressive function in melanoma cells, it abolishes tumor suppressor activity of FOXQ1.

In parallel, using a similar experimental design, we performed a reciprocal set of experiments in HMLER and SCOV3 carcinoma cells. β-catenin depletion blunted FOXQ1-dependent induction of invasion and experimental metastasis in studied carcinoma cells (Figures 5I and 5J).

Cumulatively, our data demonstrate that FOXQ1 represses *CDH2* transcription, invasion, and metastasis in the absence of nuclear β-catenin in melanoma cells, whereas FOXQ1-dependent transcriptional induction of *CDH2*, invasion, and metastasis requires activated β-catenin in carcinoma cells.

DISCUSSION

Melanoma cells with low or undetectable MITF levels comprise a prominent portion of human melanoma specimens. Understanding the mechanisms governing invasion of these cells is important for identification of melanoma targets. We demonstrate that in contrast to carcinoma cells, FOXQ1 acts as a tumor suppressor in all tested melanoma cells including those with undetectable MITF levels (SK-Mel-103, SK-Mel-147). These cells represent an excellent model for studying still poorly understood MITF-independent pathways controlling the EMT-like switch occurring in melanoma.

Several papers reported that carcinoma oncogenic EMT-TFs, SNAI2 and ZEB2, behave as tumor suppressors in melanoma cells specifically via stimulation of MITF-dependent differentiation programs (Caramel et al., 2013; Denecker et al., 2014). Our data reveal that the EMT-suppressing activities of FOXQ1 in melanoma cells rely in large part on its MITF-independent ability to repress transcription of the *CDH2* (N-cadherin) gene. Thus, unlike SNAI2 and ZEB2, the distinguishing feature of FOXQ1 tumor suppressor/oncogenic activity is that it depends on inverse regulation of the same gene in different lineage-specific contexts.

Figure 4. FOXQ1 Interacts with β-Catenin/TLE Proteins

(A) Nuclear extracts from the indicated cells were probed in immunoblotting with the indicated antibodies (TBP, TATA-binding protein).

(B) TOP:FOP luciferase reporter assay performed in the indicated cells.

(C) SK-Mel-147 cells were transduced with empty vector (V) or FOXQ1-expressing vector (F) followed by preparation of nuclear extracts, immunoprecipitation with FLAG antibodies, and immunoblotting with the indicated antibodies.

(D and E) Nuclear extracts were prepared from SK-Mel-147-FOXQ1 cells, followed by immunoprecipitation with pan-TLE (T) antibodies (D) or β-catenin (β) antibodies (E) and immunoblotting with the indicated antibodies (middle and right panels).

(F–H) Nuclear extracts were prepared from SCOV3 cells, followed by immunoprecipitation with F, FOXQ1 antibodies (F), or with T, pan-TLE antibodies (G), or with β, β-catenin antibodies (H), and immunoblotting with the indicated antibodies.

(I) SK-Mel-147 cells expressing FLAG-FOXQ1 (left) or untreated SCOV3 (right) were probed in ChIP assay with the indicated antibodies. Shown are ratios of qPCR signals in reactions with DNA precipitated with the indicated antibodies and DNA precipitated with IgG antibodies.

(J) SK-Mel-147 cells expressing FLAG-FOXQ1 (FOXQ1) or FLAG-FOXQ1 and EβP (FOXQ1+EβP) were probed in ChIP assay with antibodies indicated on the bottom. Shown are ratios of qPCR signals in reactions with DNA precipitated with the indicated antibodies and DNA precipitated with IgG antibodies.

(K) Cells were transduced with empty vector (V) or N-cadherin-expressing vector (NCAD) and superinfected with empty vector (V) or FOXQ1-expressing vector (F) and probed in immunoblotting with the indicated antibodies.

(L) Cells described in (K) were probed in invasion assay (representative chamber images are shown). Scale bars, 200 μm.

(M) Shown are invasion indexes of cells described in (K). All invasion indexes were normalized by the same in "vector-vector" cells. All data represent mean ± SEM. Statistical significance was assessed using two-tailed Student's t tests. A $p < 0.05$ (*) was considered significant.

See also Figure S4.

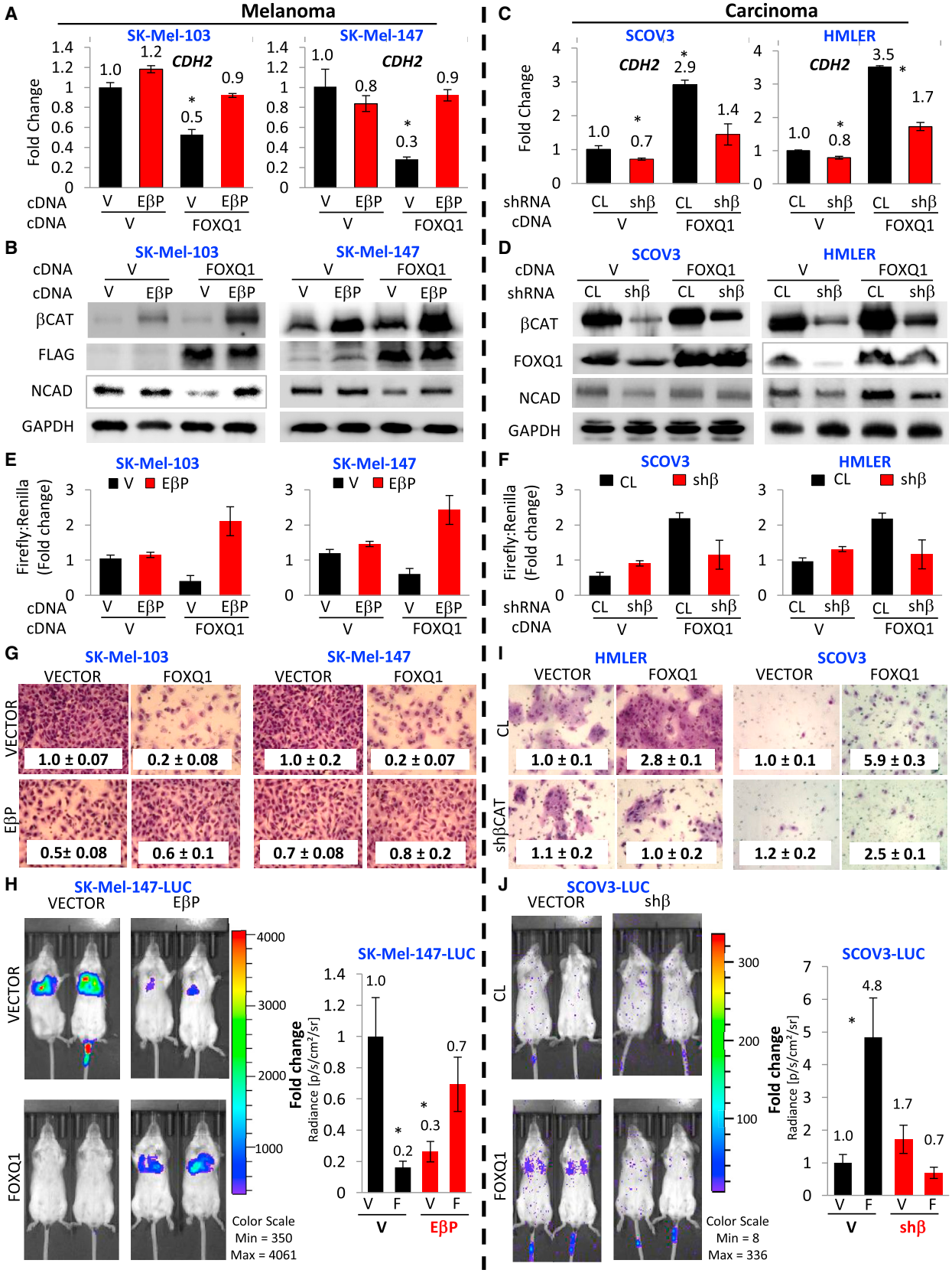

(legend on next page)

In search for nuclear determinants of the lineage-specific difference in FOXQ1 regulation of *CDH2*, we turned to β-catenin, a multifunctional protein that plays a role in cell-cell adhesion and in activation of transcription. Our data on physical interactions among FOXQ1, β-catenin, and TLE proteins in conjunction with functional interactions between FOXQ1 and β-catenin argue, for the first time, that the mode of transcriptional regulation by FOXQ1 depends on nuclear β-catenin.

Importantly, unlike in carcinomas where activation of the Wnt/β-catenin pathway is associated with increased tumorigenesis and decreased patient survival (Kahn, 2014; Novellasdemunt et al., 2015), in melanomas the role of β-catenin is controversial (Kuphal and Bosserhoff, 2011; Webster et al., 2015). The majority of studies have reported that nuclear β-catenin levels decrease in metastatic melanoma specimen and cell lines (Bachmann et al., 2005; Kuphal and Bosserhoff, 2011). It is also well established that β-catenin signaling in melanoma cells suppresses cell migration and/or invasion (Arozarena et al., 2011; Chien et al., 2009; Domingues et al., 2014). This phenomenon is attributed mostly to the β-catenin-mediated transcriptional activation of the MITF gene (Arozarena et al., 2011; Gallagher et al., 2013; Widlund et al., 2002), although MITF-independent suppression of melanoma cell migration by β-catenin has also been reported (Gallagher et al., 2013).

Our data suggest that loss of β-catenin in the course of melanoma progression should associate with the decrease in the levels of FOXQ1, which otherwise, in the absence of β-catenin, would suppress melanomagenesis. Because FOXQ1 has been reported as β-catenin transcriptional target (Peng et al., 2015) at least in carcinoma cells, the above scenario appears to be likely.

Despite multiple FOXQ1-responsive genes undergoing *CDH2*-like regulation in melanoma and carcinoma cells, suppression of *CDH2* alone is in large part responsible for invasion inhibition by FOXQ1 as was evidenced by N-cadherin reconstitution experiments (Figures 4K–4M). Direct transcriptional upregulation of *CDH2* and/or suppression of *CDH1* (E-cadherin) are considered the major events in promotion of EMT and invasion by several EMT transcription factors other than FOXQ1 such as TWIST1 and ZEB2 (Heerboth et al., 2015; Kalluri and Weinberg, 2009; Lamouille et al., 2014; Nieto et al., 2016). However, FOXQ1 did not alter TWIST1 or ZEB2, whereas E-cadherin did not express in studied cells (Figure 3A). Thus, the above factors are unlikely to account for FOXQ1-dependent suppression of invasion in melanoma cells.

Taken together, our data provide a mechanistic explanation to the opposite roles of FOXQ1 in regulation of *CDH2* gene, invasion, and metastasis in melanoma versus carcinoma cells and reveal interplay between FOXQ1 and β-catenin, two nuclear factors negating each other's tumor suppressor activity in melanoma cells while enhancing each other's oncogenic properties in carcinoma cells.

EXPERIMENTAL PROCEDURES

Cell Culture and Reagents

Melanoma cell lines SK-Mel-19, SK-Mel-28, SK-Mel-29, SK-Mel-94, SK-Mel-103, SK-Mel-147, SK-Mel-173, and G-361 were obtained from Memorial Sloan Kettering Cancer Center and cultured in DMEM supplemented with 10% fetal bovine serum, 2 mM glutamine, and 1% penicillin-streptomycin antibiotics. Populations of normal human melanocytes (NHM) were purchased from Invitrogen and maintained in Medium 254 (Invitrogen) supplemented with human melanocyte growth supplement (Invitrogen). Colo679, UACC-257, WM1366, SCOV3, and HeLa were purchased from ATCC. HMLE and HMLER cells were a gift from Dr. Robert A Weinberg (Whitehead Institute).

Immunohistochemistry

This study was approved by the Roswell Park Cancer Institute Institutional Review Board. Primary cutaneous melanoma specimens were studied using whole sections. Metastatic melanoma specimens were evaluated using TMAs. Formalin-fixed and paraffin-embedded melanoma tissues were stained with FOXQ1 antibodies (ab51340, Abcam) at the Pathology Core Facility (Roswell Park Cancer Institute) and visualized with the Novocastra (Newcastle, UK) PowerVision kit, followed by Fast Red (Thermo Scientific). Specimens were scored for intensity and percentage of stained cells by a board-certified pathologist. An immunohistochemistry (IHC) H-score was calculated as a product of these parameters.

RT-PCR Analysis

Total RNA was isolated from cells using the RNeasy Mini Kit (QIAGEN, Valencia, CA). cDNA was prepared using cDNA reverse transcription kit (Invitrogen).

Figure 5. FOXQ1 Regulates *CDH2*, Invasion, and Metastasis in a β-Catenin-Dependent Manner

(A) Melanoma cells were transduced with indicated constructs (V, empty vector; Eβp, constitutively active β-catenin; shβ, β-catenin shRNA), followed by probing in qRT-PCR. Shown are *CDH2/ACTB* ratios normalized to the same in the cells transduced with empty vector.

(B) Cells described in (A) were probed in immunoblotting with the indicated antibodies.

(C) Carcinoma cells were treated like melanoma cells in (A).

(D) Carcinoma cells were treated like melanoma cells in (B).

(E) Indicated cells described in (A) or (C) were co-transfected with the mixture of pGL3-CDH2 and Renilla-expressing vector or pGL3-control and Renilla-expressing vector, followed by luciferase reporter assay.

(F) Indicated cells described in (C) were treated like in (E).

(G) Melanoma cells described in (A) were probed in invasion assay (representative chamber images are shown). Numbers correspond to invasion indexes. All indexes were normalized by the same in "vector-vector" cells. Scale bars, 200 μm.

(H) Melanoma cells stably expressing luciferase were transduced with the indicated constructs, tail-vein injected into SCID mice. Mice injected with the same types of cells were simultaneously imaged 2–4 weeks post-injection and quantified for tumor burden.

(I) Carcinoma cells described in (C) were probed in invasion assay (representative chamber images are shown). Numbers correspond to invasion indexes. All indexes were normalized by the same in "vector-vector" cells. Scale bars, 200 μm.

(J) Carcinoma cells stably expressing luciferase were transduced with the indicated constructs, tail-vein injected into SCID mice (n = 5 mice). Mice injected with the same types of cells were simultaneously imaged 2–4 weeks post-injection and quantified for tumor burden. All data represent mean ± SEM. Statistical significance was assessed using two-tailed Student's t tests. A $p < 0.05$ (*) was considered significant.

See also Figure S5.

qRT-PCR was performed using 7900HT Fast Real-Time PCR System (Applied Biosystems, Carlsbad, CA) using SYBr GreenMaster Mix (Invitrogen). For primer sequences, see Table S2.

RNA-Seq Assay

The sequencing libraries are prepared with the TruSeq Stranded Total RNA kit (Illumina), from 1 μg total RNA according to the manufacturer's instructions. Raw reads that passed the Illumina RTA quality filter were first pre-processed by using (1) FASTQC for sequencing base quality control, and (2) Cutadapt to remove adaptor sequences. The remaining reads were mapped to the human reference genome (hg19) and RefSeq annotation database using Tophat (Trapnell et al., 2009). A second round of quality control was performed to identify potential RNA-seq library preparation problems by examining mapped BAM files using RSeQC (Wang et al., 2012) The number of reads aligning to each gene was calculated using HTSeq (Anders et al., 2015). Differentially expressed genes were identified using DESeq2 (Love et al., 2014).

Immunoblotting

Polyvinylidene difluoride (PVDF) membranes were developed using alkaline phosphatase-conjugated secondary antibodies and signals were detected and visualized using the Alpha-Innotech FluorChem HD2 imaging system (Alpha Innotech) and quantified using ImageQuant software (GE Healthcare Life Sciences). Antibodies used included: FOXQ1 (K-12 sc-47597) and (C-9 sc-166265), MITF (Clone 5, Thermofisher, MA5-14146), GAPDH (Thermofisher, PA1-987), N-cadherin (CST, D4R1H-13116), β-catenin (CST, D10A8-8480), TLE1/2/3/4 (CST, 4681S), FLAG (Sigma, F3165) LaminA (sc-56137), VIM (sc-73258), TWIST1 (sc-15393), ZEB2 (sc-271984), E-cadherin (sc-71009), AXIN2 (ab32197), and TBP (ab51841). ChIP grade from Abcam included: H3K9ac (ab4441), H3K27me3 (ab6002), H3K4me3 (ab8580), H3K9me2 (CS200587), and RNAPol-II (ab26721).

Lentiviral Vectors

FOXQ1 ORF was PCR amplified from NHM cDNA and cloned into the lentiviral expression vector pLV-puro in frame with an N terminus flag-tag. Lentiviral expression vector containing beta-catenin cDNA (S33Y)-pcw107-V5 was a gift from Drs. David Sabatini and Kris Wood (Addgene plasmid #64616). TLE1-4 was purchased from OriGene (SC111039, RC224066, RC220536, and RC202474), Lentiviral vector containing N-cadherin was purchased from Addgene (Plasmid #38153). shRNAs targeting human FOXQ1, MITF, and pLKO-1.puro lentiviral control vectors were purchased from Sigma-Aldrich (Sigma, St. Louis, MO). pLKO.1 puro shRNA beta-catenin was a gift from Dr. Robert Weinberg (Addgene plasmid #18803).

Cell Proliferation Analysis

Cells (5×10^3/well) were seeded onto 96-well pates and grown for 24–72 hr followed by fixation and staining with 0.5% methylene blue in water/methanol (50:50). The plates were rinsed using ddH_20 and air-dried. The stain was solubilized in 200 μL of 1% SDS in PBS, and the optical density was determined at 650 nm using a fluorimeter (SpectraMax).

Chromatin Immunoprecipitation

Cultured cells (5×10^7) were fixed in 1% formaldehyde at room temperature (RT) for 15 min, followed by addition of glycine (0.125 M) for 5 min. Cells were washed with ice-cold PBS, pelleted, and resuspended in ice-cold cell lysis buffer (1% SDS, 10 mM EDTA, 50 mM Tris-HCl pH 8.1, and protease inhibitors) (EZ-ChIP kit, Millipore, CA). Samples were incubated on ice for 20 min, followed by sonication (12× for 30 s each at 30-s intervals) with a Microson (Misonix). The samples were then centrifuged at 15,000 rpm, 4°C, for 10 min. A control aliquot (whole-cell extract) was set aside and supernatants were diluted 10-fold in ChIP dilution buffer (16.7 mM Tris-HCl [pH 8.1], 167 mM NaCl, 1.1% Triton X-100, 0.01% SDS, 1.2 mM EDTA protease inhibitor) (EZ-ChIP kit, Millipore, CA). Non-specific background was removed by incubating samples with protein A/G beads for 2 hr at 4°C on a rotating platform. The pre-cleared chromatin material was incubated with anti-FLAG-conjugated beads (25 μL slurry per 1×10^6 cells) on a rotating platform overnight at 4°C followed by magnetic separation. The beads were washed and the precipitated material was de-crosslinked and treated according to the EZ-ChIP kit instructions (Millipore, CA). The DNA was recovered by column purification and quantified using QUBIT DNA HS assay kit (Invitrogen).

Immunoprecipitation

Nuclear extracts were prepared by lysing cells in 10 mM HEPES, pH7.9, 1.5 mM $MgCl_2$, 10 mM KCl, and 0.5 mM DTT followed by centrifugation at 1,500 × *g*. The pellets were resuspended in 50 mM HEPES-NaOH, pH 7.9, 300 mM NaCl, 1% (v/v) NP-40, 10 mM $MgCl_2$, and 15% glycerol, followed by centrifugation at 12,000 × *g* for 10 min and overnight incubation of the supernatants with either FLAG-specific magnetic beads, IgG, or antibodies specific to the protein of interest at 4°C. If needed, agarose A/G beads were added and the material was incubated for additional 4 hr. The beads (Flag or A/G) were washed three times with 25 mM HEPES, pH 7.9, 300 mM NaCl, 0.2% NP-40.

Generation of LUC-Containing Cells

The lentiviral vector encoding the *firefly* luciferase gene (Addgene, Plasmid #17477) was used to transduce cells. Cells were selected in puromycin for 5 days, after which cells were seeded in a 96-well plate (~1 cell/well) for clonogenic selection. 7 days later cells were analyzed using IVIS bioluminescence imaging. High and consistent luciferase expressing cells were selected and serially expanded in puromycin containing media. No differences in luminescence intensity or variability were observed for cells grown with or with continued puro-selection.

Animal Studies Using a Subcutaneous Xenograft Model

Cells ($1–5 \times 10^6$) were inoculated subcutaneously in both flanks of 4- to 6-week-old female SCID mice (strain: C.B-Igh-1bIcrTac-Prkdcscid/Ros, bred and maintained by the in-house transgenic mouse facility at RPCI; n = 5 per group). Mice were monitored daily until the experiment reached its endpoint. Tumor burden was measured using calipers and volume was determined using the formula V = 0.5 (length) × (width^2). Mice were euthanized when tumor volume reached 2 cm^3, when a tumor became ulcerated, or if the mice displayed any morbidity. While the animals were not randomized after the injections, the animals were coded to blind the investigator until the experimental endpoint was reached.

IVIS Imaging

1×10^6 cells stably expressing *firefly* luciferase were injected via the tail vein into 4- to 6-week-old female SCID mice. 2–4 weeks later, bioluminescence imaging was performed using the IVIS imaging platform for assessment of tumor burden. During each imaging session, mice were anesthetized using isoflurane and intraperitoneally injected with D-luciferin (150 mg/kg). Mice were positioned uniformly within the imaging platform. Imaging was performed in 2-min intervals starting 4 min post injection for 3–4 intervals. Total flux ($p\ s^{-1}$) in the regions of interest was measured. Image acquisition and bioluminescence imaging data analysis were done with Living Image 4.0 Software (PerkinElmer). The signal intensity of tumor burdens expressed as total photons/s/cm^2 (p/s/cm^2/sr) was normalized and data were represented as fold change in tumor burden.

Luciferase Assay

The *CDH2* promoter region (−2,200:500 bp) was synthesized using GeneArt synthesis (Thermo Fisher Scientific, GeneArt) followed by sub-cloning into a pGL3-basic firefly luciferase vector (Promega, Madison, WI) generating pGL3-CDH2. The obtained constructs were mixed with pRLSV40 plasmid expressing the *Renilla* luciferase gene (Promega). Cells were transfected in triplicates with the plasmid mixtures, using SuperFect reagent (QIAGEN). Approximately 48 hr after transfection, *Firefly* luciferase and *Renilla* signals were detected according to manufacturer's instructions via Dual-Luciferase Assay Kit (Promega). *Firefly* luciferase signals were normalized by corresponding *Renilla* signals to control for transfection efficiency.

TOP-FLASH/FOP-FLASH Reporter Assay

The reporter assay consisted of a lentiviral-TOP-dGFP-reporter, a gift from Dr. Tannishtha Reya (Addgene plasmid # 14715) (Reya et al., 2003) (harboring

three β-catenin binding sites upstream of the TCF promoter) and a M51 Super 8x FOP-Flash (TOP-Flash mutant) (Veeman et al., 2003), a gift from Dr. Randall Moon (Addgene plasmid # 12457) (harboring three mutant β-catenin binding sites). The latter was used as a control for the background luciferase signal due to non-specific binding. Cells were transfected with reporter constructs including plasmid expressing the *Renilla* luciferase gene (Promega) and harvested 24–48 hr later followed by measurement of luciferase activities using dual luciferase reporter assay system as per manufacturer's instructions (Dual Glo Reporter Assay, Promega).

Matrigel Invasion Assay

Cells (1–5 × 10^3) were seeded in serum-free media onto polycarbonate 8-μm inserts (migration) and Matrigel coated-insert (invasion) (BD Bioscience, San Jose, CA). Serum-containing media was added at the bottom. Cells were incubated overnight (o/n) at 37°C, and cells in the top chamber were wiped off. Cells on the underside of the insert were fixed and stained using Diff-quick stain (VWR Scientific, West Chester, PA). The inserts were imaged at five random fields at 20× magnification followed by determination of invasion index (ratio of migration/invasion).

Statistical Analysis

Each experiment was performed at least twice with consistent results. For in vitro studies, statistical significance was determined using Student's t test. A two-tailed p value ≤ 0.5 was considered significant for all analyses. For animal studies, sample size was determined as a function of effect size ((difference in means)/(SD) = 2.0) for a two-sample t test comparison assuming a significance level of 5%, a power of 90%, and a two-sided t test. Normal distribution was confirmed using normal probability plot (GraphPad Prism 6.0, GraphPad Software, San Diego, CA), variance was also assessed using GraphPad Prism 6.0, both within and between groups, and were approximately the same. For statistically analysis of immunohistological scores, an unpaired Student's t test was used and a value of $p \leq 0.05$ was considered statistically significant.

ACCESSION NUMBERS

The accession number for the RNA-seq data reported in this paper is GEO: GSE103071.

SUPPLEMENTAL INFORMATION

Supplemental Information includes Supplemental Experimental Procedures, five figures, and two tables and can be found with this article online at http://dx.doi.org/10.1016/j.celrep.2017.08.057.

AUTHOR CONTRIBUTIONS

A.B. and M.A.N. designed the experiments and wrote the manuscript. A.B., A.B.-S., S.M., K.K., E.E.F., B.C.L., M.K., P.J., A.P., A.M., J.R., J.A.W., D.H.Y., N.I.K., J.W., and S.L. performed experiments and analyzed the data. S.L., A.E.B., G.P., and M.J.N. advised on the experiments. M.A.N. designed the experiments, analyzed the data, and supervised the study. All authors discussed the results and commented on the manuscript.

ACKNOWLEDGMENTS

We are grateful to Dr. Dominic Smiraglia for critical reading of the manuscript, to the Pathology Resource Network, the Clinical Data Network, and the transgenic shared core facility (funded by NCI P30CA16056) at Roswell Park Cancer Institute. This work has been supported by NCI (CA190533, CA193981, and CA202162 to M.A.N.).

Received: July 2, 2017
Revised: August 11, 2017
Accepted: August 17, 2017
Published: September 19, 2017

REFERENCES

Alonso, S.R., Tracey, L., Ortiz, P., Pérez-Gómez, B., Palacios, J., Pollán, M., Linares, J., Serrano, S., Sáez-Castillo, A.I., Sánchez, L., et al. (2007). A high-throughput study in melanoma identifies epithelial-mesenchymal transition as a major determinant of metastasis. Cancer Res. *67*, 3450–3460.

Anders, S., Pyl, P.T., and Huber, W. (2015). HTSeq–a Python framework to work with high-throughput sequencing data. Bioinformatics *31*, 166–169.

Arozarena, I., Bischof, H., Gilby, D., Belloni, B., Dummer, R., and Wellbrock, C. (2011). In melanoma, beta-catenin is a suppressor of invasion. Oncogene *30*, 4531–4543.

Bachmann, I.M., Straume, O., Puntervoll, H.E., Kalvenes, M.B., and Akslen, L.A. (2005). Importance of P-cadherin, β-catenin, and Wnt5a/frizzled for progression of melanocytic tumors and prognosis in cutaneous melanoma. Clin. Cancer Res. *11*, 8606–8614.

Bianchi-Smiraglia, A., Bagati, A., Fink, E.E., Moparthy, S., Wawrzyniak, J.A., Marvin, E.K., Battaglia, S., Jowdy, P., Kolesnikova, M., Foley, C.E., et al. (2017). Microphthalmia-associated transcription factor suppresses invasion by reducing intracellular GTP pools. Oncogene *36*, 84–96.

Biechele, T.L., Kulikauskas, R.M., Toroni, R.A., Lucero, O.M., Swift, R.D., James, R.G., Robin, N.C., Dawson, D.W., Moon, R.T., and Chien, A.J. (2012). Wnt/β-catenin signaling and AXIN1 regulate apoptosis triggered by inhibition of the mutant kinase BRAFV600E in human melanoma. Sci. Signal. *5*, ra3.

Caramel, J., Papadogeorgakis, E., Hill, L., Browne, G.J., Richard, G., Wierinckx, A., Saldanha, G., Osborne, J., Hutchinson, P., Tse, G., et al. (2013). A switch in the expression of embryonic EMT-inducers drives the development of malignant melanoma. Cancer Cell *24*, 466–480.

Carreira, S., Goodall, J., Denat, L., Rodriguez, M., Nuciforo, P., Hoek, K.S., Testori, A., Larue, L., and Goding, C.R. (2006). Mitf regulation of Dia1 controls melanoma proliferation and invasiveness. Genes Dev. *20*, 3426–3439.

Chien, A.J., Moore, E.C., Lonsdorf, A.S., Kulikauskas, R.M., Rothberg, B.G., Berger, A.J., Major, M.B., Hwang, S.T., Rimm, D.L., and Moon, R.T. (2009). Activated Wnt/β-catenin signaling in melanoma is associated with decreased proliferation in patient tumors and a murine melanoma model. Proc. Natl. Acad. Sci. USA *106*, 1193–1198.

Christensen, J., Bentz, S., Sengstag, T., Shastri, V.P., and Anderle, P. (2013). FOXQ1, a novel target of the Wnt pathway and a new marker for activation of Wnt signaling in solid tumors. PLoS ONE *8*, e60051.

Daniels, D.L., and Weis, W.I. (2005). Beta-catenin directly displaces Groucho/TLE repressors from Tcf/Lef in Wnt-mediated transcription activation. Nat. Struct. Mol. Biol. *12*, 364–371.

Denecker, G., Vandamme, N., Akay, O., Koludrovic, D., Taminau, J., Lemeire, K., Gheldof, A., De Craene, B., Van Gele, M., Brochez, L., et al. (2014). Identification of a ZEB2-MITF-ZEB1 transcriptional network that controls melanogenesis and melanoma progression. Cell Death Differ. *21*, 1250–1261.

Domingues, M.J., Rambow, F., Job, B., Papon, L., Liu, W., Larue, L., and Bonaventure, J. (2014). β-catenin inhibitor ICAT modulates the invasive motility of melanoma cells. Cancer Res. *74*, 1983–1995.

Domingues, M.J., Martinez-Sanz, J., Papon, L., Larue, L., Mouawad, L., and Bonaventure, J. (2017). Structure-based mutational analysis of ICAT residues mediating negative regulation of beta-catenin co-transcriptional activity. PLoS One *12*, e0172603.

Gallagher, S.J., Rambow, F., Kumasaka, M., Champeval, D., Bellacosa, A., Delmas, V., and Larue, L. (2013). Beta-catenin inhibits melanocyte migration but induces melanoma metastasis. Oncogene *32*, 2230–2238.

Garraway, L.A., Widlund, H.R., Rubin, M.A., Getz, G., Berger, A.J., Ramaswamy, S., Beroukhim, R., Milner, D.A., Granter, S.R., Du, J., et al. (2005). Integrative genomic analyses identify MITF as a lineage survival oncogene amplified in malignant melanoma. Nature *436*, 117–122.

Hartman, M.L., and Czyz, M. (2015). MITF in melanoma: mechanisms behind its expression and activity. Cell. Mol. Life Sci. *72*, 1249–1260.

Heerboth, S., Housman, G., Leary, M., Longacre, M., Byler, S., Lapinska, K., Willbanks, A., and Sarkar, S. (2015). EMT and tumor metastasis. Clin. Transl. Med. *4*, 6.

Hoek, K.S., Eichhoff, O.M., Schlegel, N.C., Döbbeling, U., Kobert, N., Schaerer, L., Hemmi, S., and Dummer, R. (2008). In vivo switching of human melanoma cells between proliferative and invasive states. Cancer Res. *68*, 650–656.

Kahn, M. (2014). Can we safely target the WNT pathway? Nat. Rev. Drug Discov. *13*, 513–532.

Kalluri, R., and Weinberg, R.A. (2009). The basics of epithelial-mesenchymal transition. J. Clin. Invest. *119*, 1420–1428.

Kuphal, S., and Bosserhoff, A.K. (2011). Phosphorylation of β-catenin results in lack of β-catenin signaling in melanoma. Int. J. Oncol. *39*, 235–243.

Lamouille, S., Xu, J., and Derynck, R. (2014). Molecular mechanisms of epithelial-mesenchymal transition. Nat. Rev. Mol. Cell Biol. *15*, 178–196.

Li, F.Z., Dhillon, A.S., Anderson, R.L., McArthur, G., and Ferrao, P.T. (2015). Phenotype switching in melanoma: implications for progression and therapy. Front. Oncol. *5*, 31.

Li, Y., Zhang, Y., Yao, Z., Li, S., Yin, Z., and Xu, M. (2016). Forkhead box Q1: a key player in the pathogenesis of tumors (Review). Int. J. Oncol. *49*, 51–58.

Love, M.I., Huber, W., and Anders, S. (2014). Moderated estimation of fold change and dispersion for RNA-seq data with DESeq2. Genome Biol. *15*, 550.

Meng, F., Speyer, C.L., Zhang, B., Zhao, Y., Chen, W., Gorski, D.H., Miller, F.R., and Wu, G. (2015). PDGFRα and β play critical roles in mediating Foxq1-driven breast cancer stemness and chemoresistance. Cancer Res. *75*, 584–593.

Nieto, M.A., Huang, R.Y., Jackson, R.A., and Thiery, J.P. (2016). EMT: 2016. Cell *166*, 21–45.

Novellasdemunt, L., Antas, P., and Li, V.S.W. (2015). Targeting Wnt signaling in colorectal cancer. a review in the theme: cell signaling: proteins, pathways and mechanisms. Am. J. Physiol. Cell Physiol. *309*, C511–C521.

Peng, X., Luo, Z., Kang, Q., Deng, D., Wang, Q., Peng, H., Wang, S., and Wei, Z. (2015). FOXQ1 mediates the crosstalk between TGF-β and Wnt signaling pathways in the progression of colorectal cancer. Cancer Biol. Ther. *16*, 1099–1109.

Qiao, Y., Jiang, X., Lee, S.T., Karuturi, R.K., Hooi, S.C., and Yu, Q. (2011). FOXQ1 regulates epithelial-mesenchymal transition in human cancers. Cancer Res. *71*, 3076–3086.

Rambow, F., Bechadergue, A., Luciani, F., Gros, G., Domingues, M., Bonaventure, J., Meurice, G., Marine, J.C., and Larue, L. (2016). Regulation of melanoma progression through the TCF4/miR-125b/NEDD9 cascade. J. Invest. Dermatol. *136*, 1229–1237.

Reya, T., Duncan, A.W., Ailles, L., Domen, J., Scherer, D.C., Willert, K., Hintz, L., Nusse, R., and Weissman, I.L. (2003). A role for Wnt signalling in self-renewal of haematopoietic stem cells. Nature *423*, 409–414.

Roose, J., Molenaar, M., Peterson, J., Hurenkamp, J., Brantjes, H., Moerer, P., van de Wetering, M., Destrée, O., and Clevers, H. (1998). The Xenopus Wnt effector XTcf-3 interacts with Groucho-related transcriptional repressors. Nature *395*, 608–612.

Salti, G.I., Manougian, T., Farolan, M., Shilkaitis, A., Majumdar, D., and Das Gupta, T.K. (2000). Micropthalmia transcription factor: a new prognostic marker in intermediate-thickness cutaneous malignant melanoma. Cancer Res. *60*, 5012–5016.

Schadendorf, D., Fisher, D.E., Garbe, C., Gershenwald, J.E., Grob, J.-J., Halpern, A., Herlyn, M., Marchetti, M.A., McArthur, G., Ribas, A., et al. (2015). Melanoma. Nat. Rev. Dis. Primers *1*, 15003.

Selzer, E., Wacheck, V., Lucas, T., Heere-Ress, E., Wu, M., Weilbaecher, K.N., Schlegel, W., Valent, P., Wrba, F., Pehamberger, H., et al. (2002). The melanocyte-specific isoform of the microphthalmia transcription factor affects the phenotype of human melanoma. Cancer Res. *62*, 2098–2103.

Shain, A.H., and Bastian, B.C. (2016). From melanocytes to melanomas. Nat. Rev. Cancer *16*, 345–358, advance online publication.

Smith, A.P., Hoek, K., and Becker, D. (2005). Whole-genome expression profiling of the melanoma progression pathway reveals marked molecular differences between nevi/melanoma in situ and advanced-stage melanomas. Cancer Biol. Ther. *4*, 1018–1029.

Trapnell, C., Pachter, L., and Salzberg, S.L. (2009). TopHat: discovering splice junctions with RNA-Seq. Bioinformatics *25*, 1105–1111.

Tulchinsky, E., Pringle, J.H., Caramel, J., and Ansieau, S. (2014). Plasticity of melanoma and EMT-TF reprogramming. Oncotarget *5*, 1–2.

Veeman, M.T., Slusarski, D.C., Kaykas, A., Louie, S.H., and Moon, R.T. (2003). Zebrafish prickle, a modulator of noncanonical Wnt/Fz signaling, regulates gastrulation movements. Curr. Biol. *13*, 680–685.

Wang, L., Wang, S., and Li, W. (2012). RSeQC: quality control of RNA-seq experiments. Bioinformatics *28*, 2184–2185.

Webster, M.R., Kugel Iii, C.H., and Weeraratna, A.T. (2015). The Wnts of change: How Wnts regulate phenotype switching in melanoma. Biochim. Biophys. Acta. *1856*, 244–251.

Wellbrock, C., and Marais, R. (2005). Elevated expression of MITF counteracts B-RAF-stimulated melanocyte and melanoma cell proliferation. J. Cell Biol. *170*, 703–708.

Wheelock, M.J., Shintani, Y., Maeda, M., Fukumoto, Y., and Johnson, K.R. (2008). Cadherin switching. J. Cell Sci. *121*, 727–735.

Widlund, H.R., Horstmann, M.A., Price, E.R., Cui, J., Lessnick, S.L., Wu, M., He, X., and Fisher, D.E. (2002). β-catenin-induced melanoma growth requires the downstream target Microphthalmia-associated transcription factor. J. Cell Biol. *158*, 1079–1087.

Zhang, H., Meng, F., Liu, G., Zhang, B., Zhu, J., Wu, F., Ethier, S.P., Miller, F., and Wu, G. (2011). Forkhead transcription factor foxq1 promotes epithelial-mesenchymal transition and breast cancer metastasis. Cancer Res. *71*, 1292–1301.

Cell Reports, Volume *20*

Supplemental Information

Melanoma Suppressor Functions of the Carcinoma Oncogene FOXQ1

Archis Bagati, Anna Bianchi-Smiraglia, Sudha Moparthy, Kateryna Kolesnikova, Emily E. Fink, Brittany C. Lipchick, Masha Kolesnikova, Peter Jowdy, Anthony Polechetti, Amin Mahpour, Jason Ross, Joseph A. Wawrzyniak, Dong Hyun Yun, Gyorgy Paragh, Nadezhda I. Kozlova, Albert E. Berman, Jianmin Wang, Song Liu, Michael J. Nemeth, and Mikhail A. Nikiforov

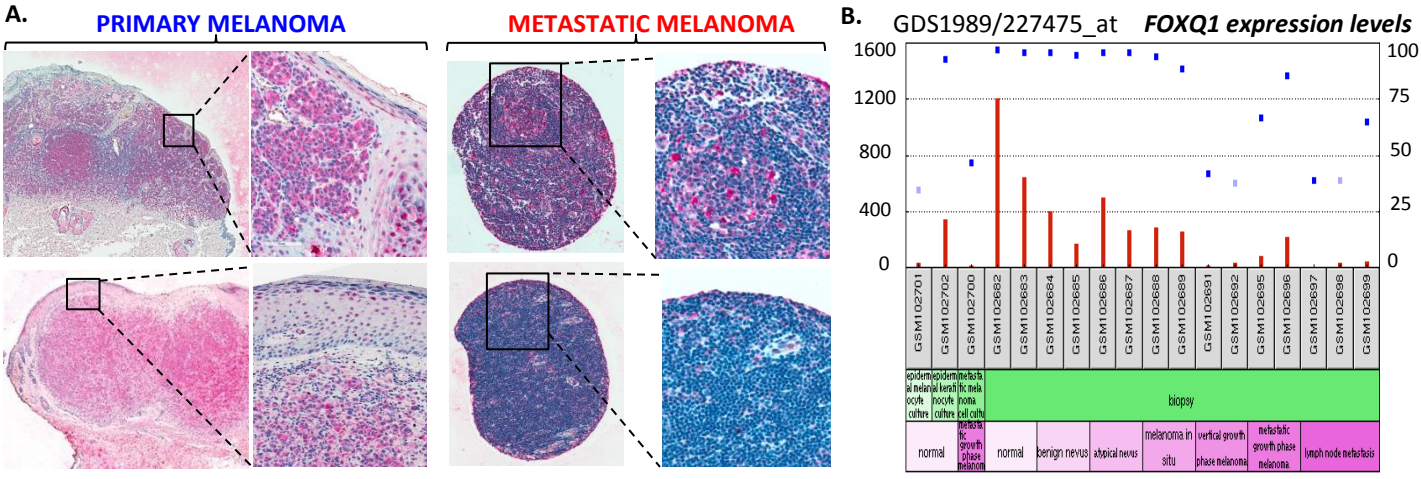

Supplemental Figure S1, related to Figure 1. FOXQ1 levels decrease in melanoma progression

A. Representative IHC images of FOXQ1 staining in primary and metastatic melanoma samples. See Methods for sample description and analysis. **B.** Expression levels of *FOXQ1* (probe ID shown) in tissue specimens representing different stages of melanoma progression derived from the publically available dataset GSE4587.

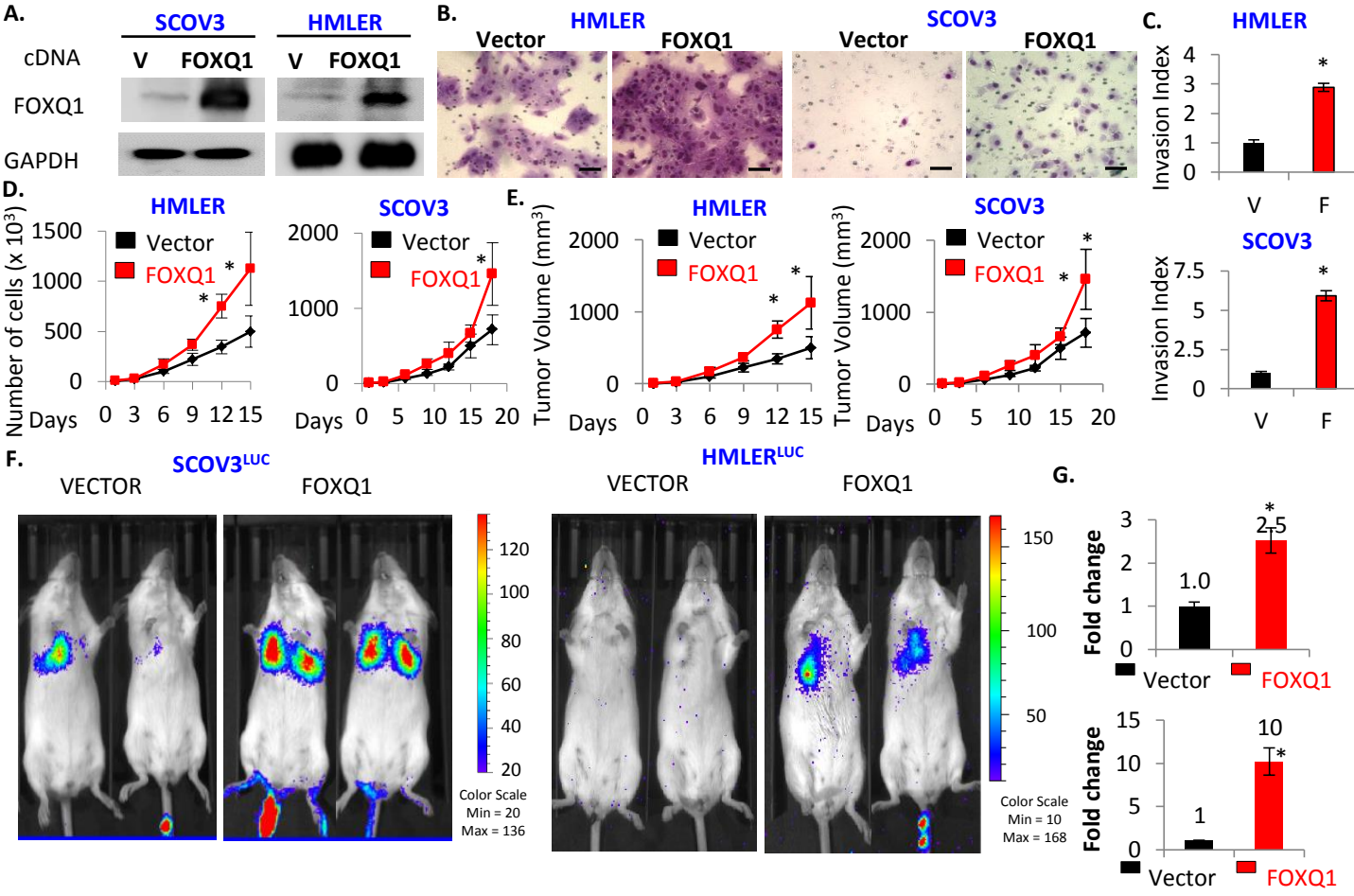

Supplemental Figure S2, related to Figure 2. FOXQ1 induces transformed phenotypes in carcinoma cells

A. Cells were transduced with the indicated constructs, followed by immunoblotting with the indicated antibodies. B. Representative images of cells described in (A) after completion of Boyden invasion chambers assay. Scale bars 200µm. C. Quantification of invasion assay in (B). D. Cells described in (A) were counted on indicated days starting 48hrs after infection. E. Cells described in (A) were subjected to tumorigenicity assay in SCID mice, (n=5, two injection sites per mouse). Tumor measurements were done at indicated days post-injection. F. SCOV3LUC and HMLERLUC cells stably expressing luciferase were transduced with the indicated constructs and injected via the tail-vein (1x106 cells) into SCID mice (n=6 per cell line). Three weeks later mice were subjected to bioluminescence detection using the IVIS imaging platform. Representative mice are shown. G. Total metastatic burden was measured using IVIS and analyzed. All data represent mean ± s.e.m. Statistical significance was assessed using two-tailed Student's t-tests. A $p<0.05$ (*) was considered significant.

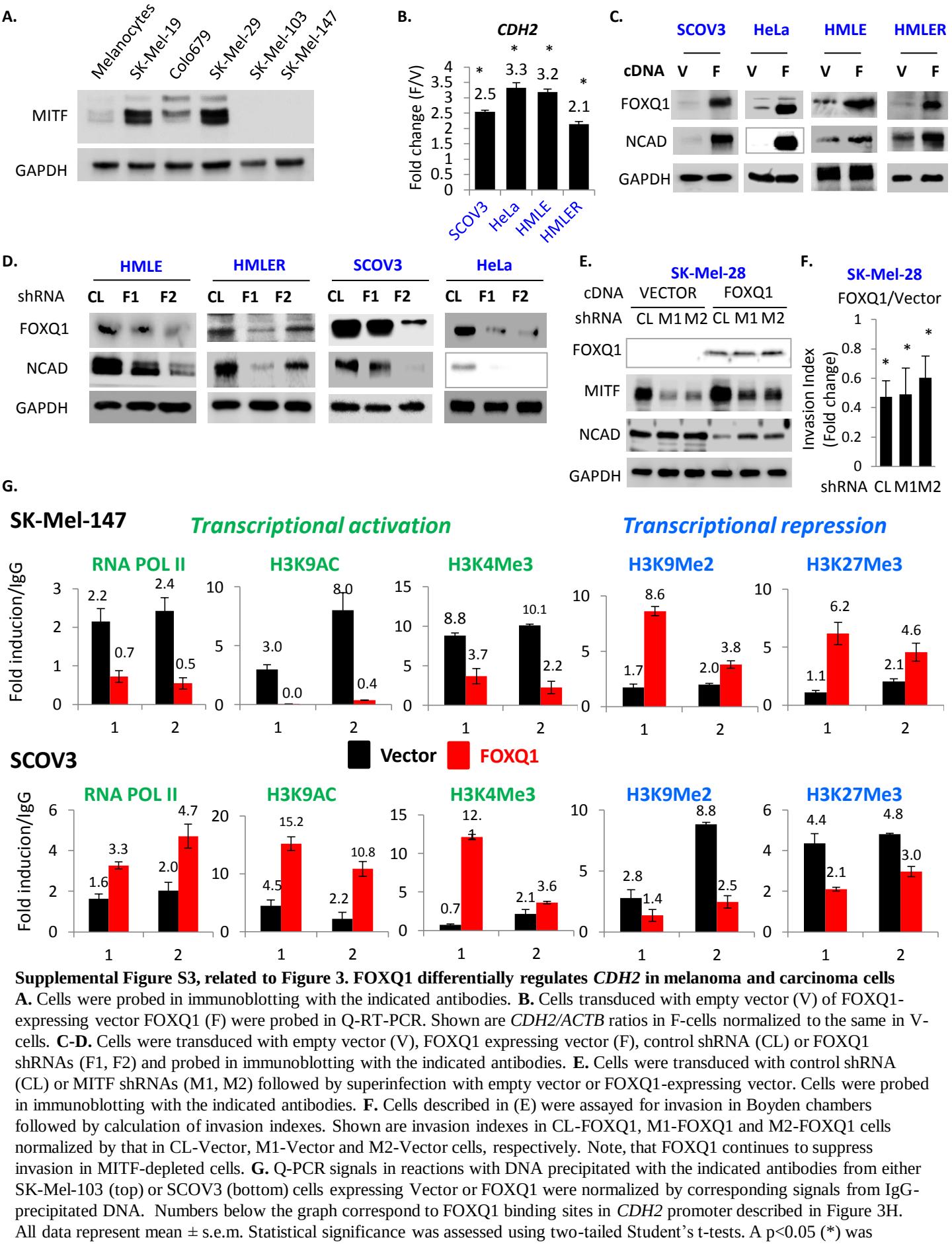

Supplemental Figure S3, related to Figure 3. FOXQ1 differentially regulates *CDH2* in melanoma and carcinoma cells
A. Cells were probed in immunoblotting with the indicated antibodies. **B.** Cells transduced with empty vector (V) of FOXQ1-expressing vector FOXQ1 (F) were probed in Q-RT-PCR. Shown are *CDH2/ACTB* ratios in F-cells normalized to the same in V-cells. **C-D.** Cells were transduced with empty vector (V), FOXQ1 expressing vector (F), control shRNA (CL) or FOXQ1 shRNAs (F1, F2) and probed in immunoblotting with the indicated antibodies. **E.** Cells were transduced with control shRNA (CL) or MITF shRNAs (M1, M2) followed by superinfection with empty vector or FOXQ1-expressing vector. Cells were probed in immunoblotting with the indicated antibodies. **F.** Cells described in (E) were assayed for invasion in Boyden chambers followed by calculation of invasion indexes. Shown are invasion indexes in CL-FOXQ1, M1-FOXQ1 and M2-FOXQ1 cells normalized by that in CL-Vector, M1-Vector and M2-Vector cells, respectively. Note, that FOXQ1 continues to suppress invasion in MITF-depleted cells. **G.** Q-PCR signals in reactions with DNA precipitated with the indicated antibodies from either SK-Mel-103 (top) or SCOV3 (bottom) cells expressing Vector or FOXQ1 were normalized by corresponding signals from IgG-precipitated DNA. Numbers below the graph correspond to FOXQ1 binding sites in *CDH2* promoter described in Figure 3H. All data represent mean ± s.e.m. Statistical significance was assessed using two-tailed Student's t-tests. A $p<0.05$ (*) was considered significant

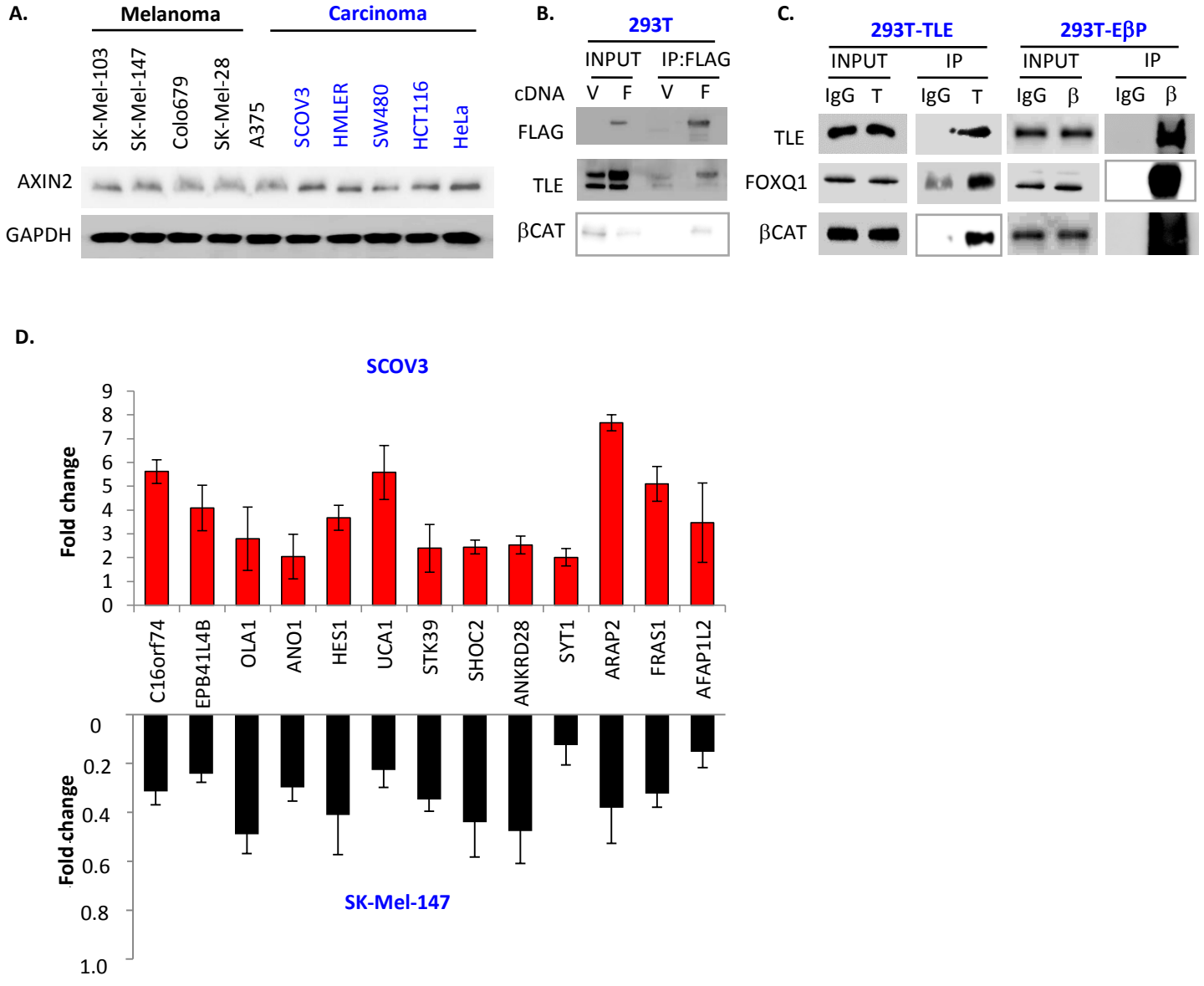

Supplemental Figure S4, related to Figure 4. FOXQ1 interacts with β-catenin/TLE proteins

A. Indicated cells were probed in immunoblotting with indicated antibodies. **B.** HEK293T cells were transfected with empty vector (V) or FLAG-FOXQ1-expressing vector (F), followed by preparation of nuclear extracts, immunoprecipitation with FLAG antibodies and probing in immunoblotting with the indicated antibodies. **C.** HEK293T cells were transfected with a mixture of TLE1-4 cDNAs (TLE) or EβP, followed by preparation of nuclear extracts, immunoprecipitation with IgG, pan-TLE (T) or β-catenin (β) antibodies and probing in immunoblotting with the indicated antibodies. **D.** SCOV3 cells (top) and SK-Mel-147 cells (bottom) were transduced with empty vector or FOXQ1-expressing vector and probed in Q-RT-PCR. Shown are ratios of a gene-specific signal to *ACTB*-specific signal in FOXQ1-expressing cells normalized to the same in cells transduced with empty vector

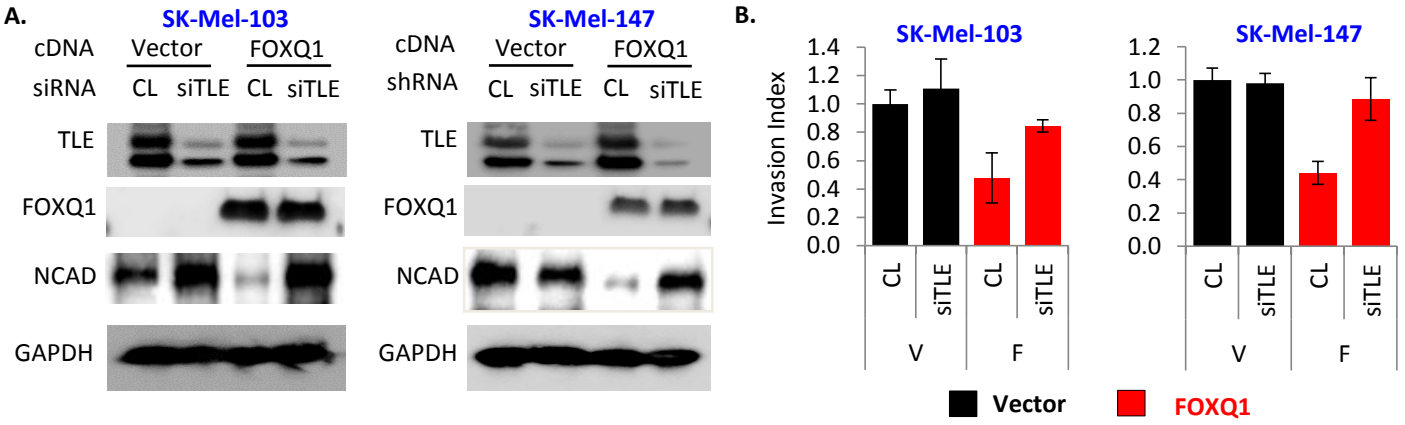

Supplemental Figure S5, related to Figure 5. TLE depletion counteracts FOXQ1-dependent suppression of N-cadherin and invasion

A. Cells transduced with empty vector (Vector) or FOXQ1-expressing vector (FOXQ1) were transfected with control siRNA (CL) or mixture of siRNAs against *TLE-1*, *-2*, *-3*, and *-4* (siTLE). Cells were probed in immunoblotting with the indicated antibodies. **B.** Cells described in (A) were probed in invasion assay. Shown are invasion indexes of cells described in (A) normalized by the same in vector cells.